Semi-Circle Theorem of Unstable Spectrum Distribution of Heterotropic Perturbation and the Upper Bound Estimation of Its Growth Rate①

Zhang Ming (张 铭) and Zhang Lifeng (张立凤)

Meteorological College, P.L.A. University of Science and Technology, Nanjing, 211101

(Received December 1, 2000; revised April 10, 2001)

ABSTRACT

Based on the theoretical analysis on the unstable spectrum distribution of heterotropic perturbation, the semi-circle theorem of such spectrum distribution is obtained — the spectrum distributed within an upper semi-circle domain with radius R_0 and taking origin as its circle center in the complex plane, and the upper bound estimation of growth rate is given simultaneously. It is found that the smaller the horizontal scale of perturbation is, the higher the model top located, the greater the estimated value of upper bound of such growth rate is. Also the increase of vertical shear of wind and latitude have the positive contribution to the increase of such growth rate. Finally when stratified stability decreases, the relative maximal growth rate increases, while the maximal growth rate decreases instead.

Key words: Heterotropic perturbation, Semi-circle theorem, Growth rate

1. Introduction

As an important study of atmospheric dynamics, the instability of mesoscale perturbation has attracted the attention of many scientists to study on such theme which both discovers the physical essence of atmospheric motion and provides the theoretical foundation for the improvement of real prediction. Until now, the main study domain of mesoscale dynamic instability still focus on two aspects — symmetry instability and transversal wave instability.

Symmetry instability is also called slantwise ascending instability or slantwise convective instability. The study of such instability aims initially at the explanation of large-scale convection in planetary circulation and then it is applied into the research of trigger mechanism of some mesoscale weather phenomenon (such as mid-latitude squall line, frontal precipitation, rain belt and blizzard etc.). Zhang (1988a, b) obtained the dispersion relation with rigid boundary condition and achieved the conclusion that the symmetry instability can be caused only in the case of $0 < Ri < 1$ (Ri is Richardson number) excluding the horizontal shear of basic stream. In recent years, Bennetts, Hoskins, Emanuel, Xu Qin and many others have studied the symmetry instability and revealed that such instability may be of great importance in organizing and starting up band convection, giving a rational explanation to multiple rain belts appearing in fronts and cyclones. From the early study on relation between

①The initial study on the instability of such perturbation is mainly supported by National Special Key Project Fund (No. G1998040907) and National Natural Science Foundation of China under Grant No. 49875008.

WAVE–CISK and symmetry instability subjected to non–static equilibrium (Zhang and Zhang, 1992), it is found that propagating unstable perturbation will appear once where heating takes place. Furthermore, with a non–static model of quasi–two dimensions, numerical method is applied in the study of the effect of heating feedback to linear and non–linear symmetry instability (Zhang and Zhang, 1995).

Perturbation propagating along the basic stream (its equal phase plane is perpendicular to basic stream) is defined as transversal perturbation. The initial study on the instability of such perturbation is mainly concentrated on synoptic and convective scale. Baroclinic instability — the instability found by Charney (1947) and Eady (1949) and the eddy mode of synoptic scale and subsynoptic scale is obtained. Zhang (1988a, b) achieved the double–mode unstable spectrum of baroclinic stream through extending eddy mode from f–plane to non–geostrophic case. Possessing the quasi–geostrophic character, eddy mode appeared in synoptic and subsynoptic scale which belongs to baroclinic instability is the final reason of the causing and developing of long wave perturbation in mid– and high latitude. While non–geostrophic mesoscale mode appears in tens or hundreds kilometers scale and non–symmetry cat eyes pattern appears in its vertical cross–section. As to the same linear wind profile, the developing of mesoscale mode is 4 times that of Eady mode, then the strong vertical motion and low–level convergence can be caused by such great growth rate, and the deep convection clouds group can be started up and organized in further step. Thus, the instability of mesoscale mode is defined as transversal instability by Zhang (1988a, b) and we have given some other studies on transversal instability and the effect of condensation heating to it and further regarded it as an initial value problem and the numerical experiment was given on it (Zhang and Zhang, 1998).

Xu and Wang (1989) has analyzed 33 times the radar observation of rain belt ahead of cold front in China and drawn out 3 different types of mesoscale rain belt in warm region — parallel, perpendicular and heterotropic one. Hereinto the relation between the parallel and the symmetry instability has been proved well, and the perpendicular case can be explained by transversal instability. Many cloud belts and rain belts which are heterotropic to basic stream have been observed during the mesoscale experiments in East China. All the above facts show that many clouds and rain belts in real atmosphere are neither parallel nor perpendicular to the basic stream but heterotropic to it, and so its cause and development couldn't be explained by the theory of symmetry instability or transversal one. Thus, it is of great real significance to study the unstable mechanism of such heterotropic perturbation, and symmetry instability transversal instability and large–scale baroclinic instability are all the special cases of such heterotropic one.

Recently, the instability of such heterotropic perturbation was studied and some analyses on its characteristics, structure and energy transformation (Zhang and Zhang, 2000) were given. A linear, non–viscous and adiabatic Boussinesq equations set in f–plane is adopted with supposing, the basic stream is merely the function of height z, and there exists an angle α between basic stream and perturbation propagating direction and the perturbation is homogeneous in y direction. This instability problem can be transformed as an eigenvalue problem of ordinary differential equation set with complex variable coefficients. After giving the solution pattern and upper and lower rigid boundary conditions, such problem can be further transformed as an eigenvalue problem of complex matrix through numerical method, and its solution can be obtained. The analysis on its eigenvalue gives the growth rate, phase speed and spectrum distribution of perturbation, while the analysis on its eigenvector gives the structure

of perturbation. Now, it is obvious that estimating the spectrum distribution and the upper bound of growth rate of such heterotropic instability and discussing the effect of environmental factor to them in theory are all of great importance and this paper would cover these aspects.

2. Mathematical model

Here, we adopt a linear, non-viscous and adiabatic Boussinesq equation set in f-plane (Wang, 2000) assuming the basic stream U is merely a linear function of height z, and there exists a constant angle α between basic stream and the propagating direction of disturbance (x direction) which is homogeneous in y direction. Until now, we get, $\bar{u} = \bar{U}\cos\delta$, $\bar{v} = \bar{U}\sin\delta$. Here $\bar{U} = |U|$, it is a linear function of z, and δ is a constant, and as a linear function of z, u, and $\bar{v}$, are components in x axis and y axis of basic stream. After taking the mass stream function ψ of perturbation and eliminating the perturbation pressure, we get

$$\begin{cases} (\frac{\partial}{\partial t} + \bar{u}\frac{\partial}{\partial x})v + f\frac{\partial \psi}{\partial z} - \frac{d\bar{v}}{dz}\frac{\partial \psi}{\partial x} = 0, \\ (\frac{\partial}{\partial t} + \bar{u}\frac{\partial}{\partial x})\theta + f\frac{\partial \psi}{\partial z}\frac{d\bar{v}}{dz} - fv\frac{d\bar{u}}{dz} - N^2\frac{\partial \psi}{\partial x} = 0, \\ (\frac{\partial}{\partial t} + \bar{u}\frac{\partial}{\partial x})\nabla^2\psi - f\frac{\partial v}{\partial z} + \frac{\partial \theta}{\partial x} = 0 \end{cases} \tag{1}$$

Here $(u, v, w, \theta) \equiv \bar{\rho}(u', v', w', \frac{g}{\theta_0}\theta')$, $u = \frac{\partial \psi}{\partial z}$, $w = -\frac{\partial \psi}{\partial x}$, $\nabla^2 = \frac{\partial^2}{\partial x^2} + \frac{\partial^2}{\partial z^2}$, N^2 is stratified parameter, $N^2 > 0$ exists all through the paper, and other symbols are same as generally used in meteorology. Considering upper and lower rigid boundary conditions with ignoring the terrain, the following condition can be achieved

$$\psi|_{z=0} = 0, \quad \psi|_{z=H} = 0 \tag{2}$$

Here H is the height of model top and generally takes the height of tropopause (about 10 km) or inversion lid. Let the wave solution has the following pattern

$$\begin{bmatrix} v \\ \theta \\ \psi \end{bmatrix} = \begin{bmatrix} \mathrm{i}V(z) \\ \Theta(z) \\ \Psi(z) \end{bmatrix} \mathrm{e}^{\mathrm{i}(kx - \sigma t)} \tag{3}$$

and introducing it into Equation (1), after dividing the two sides of equation with k, we achieve the next step. Taking $\tilde{f} = f/k$ and $c = \sigma/k$, the following equations can be obtained

$$\begin{cases} (\bar{u} - c)V + \mathrm{i}\Psi\frac{d\bar{v}}{dz} - \tilde{f}\frac{d\Psi}{dz} = 0, \\ (\bar{u} - c)\Theta - N^2\Psi - \mathrm{i}\tilde{f}\frac{d\bar{v}}{dz}\frac{d\Psi}{dz} - \tilde{f}\frac{d\bar{u}}{dz}V = 0, \\ (\bar{u} - c)(\frac{d^2\Psi}{dz^2} - k^2\Psi) - \tilde{f}\frac{dV}{dz} + \Theta = 0 \end{cases} \tag{4}$$

with its boundary condition as

$$\Psi|_{z=0} = 0, \quad \Psi|_{z=H} = 0. \tag{5}$$

After eliminating V and Θ, the following expression can be achieved

$$(\bar{u}-c)\left[(\bar{u}-c)^2-\hat{f}^2\right]\frac{d^2\Psi}{dz^2}+2\left[i\hat{f}(\bar{u}-c)\frac{d\bar{v}}{dz}+\hat{f}^2\frac{d\bar{u}}{dz}\right]\frac{d\Psi}{dz}$$
$$+\left\{(\bar{u}-c)\left[N^2-k^2(\bar{u}-c)^2\right]-2\hat{f}i\frac{du}{dz}\frac{d\bar{v}}{dz}\right\}\Psi=0. \tag{6}$$

Together with boundary condition (5), Equation (6) constitutes an eigenvalue problem of ordinary differential equations set with complex varying coefficients.

3. Semi-circle theorem and the upper bound of growth rate of heterotropic instability

Let $\bar{u}-c=\lambda$ (λ is a function of z), then Formula (6) can be written as

$$\lambda(\lambda^2-\hat{f}^2)\frac{d^2\Psi}{dz^2}+2(i\hat{f}\lambda\bar{v}_z+\hat{f}^2\bar{u}_z)\frac{d\Psi}{dz}+[\lambda(N^2-k^2\lambda^2)-2\hat{f}i\bar{u}_z\bar{v}_z]\Psi=0. \tag{7}$$

Here $\bar{u}_z=\frac{d\bar{u}}{dz}=\frac{d\bar{U}}{dz}\cos\delta=\bar{U}_z\cos\delta$, and $\bar{v}_z=\frac{d\bar{v}}{dz}=\frac{d\bar{U}}{dz}\sin\delta=\bar{U}_z\sin\delta$, when there exists instability, c is a complex number and $\lambda\neq0$, then

$$\frac{d^2\Psi}{dz^2}+\left[\frac{2i\hat{f}\bar{v}_z}{\lambda^2-\hat{f}^2}+\frac{2\hat{f}^2\bar{u}_z}{\lambda(\lambda^2-\hat{f}^2)}\right]\frac{d\Psi}{dz}+\left[\frac{N^2-k^2\lambda^2}{\lambda^2-\hat{f}^2}-\frac{2\hat{f}i\bar{u}_z\bar{v}_z}{\lambda(\lambda^2-\hat{f}^2)}\right]\Psi=0. \tag{8}$$

After being multiplied by Ψ^* and integrated in $[0, H]$, and consider condition (5), Formula (8) can be transformed as

$$\int_0^H\left[\frac{2i\hat{f}\bar{v}_z}{\lambda^2-\hat{f}^2}+\frac{2\hat{f}^2\bar{u}_z}{\lambda(\lambda^2-\hat{f}^2)}\right]\Psi^*\frac{d\Psi}{dz}dz+\int_0^H\left[\frac{N^2-k^2\hat{f}^2}{\lambda^2-\hat{f}^2}-\frac{2\hat{f}i\bar{u}_z\bar{v}_z}{\lambda(\lambda^2-\hat{f}^2)}\right]|\Psi|^2dz$$
$$=\int_0^H\left|\frac{d\Psi}{dz}\right|^2dz+k^2\int_0^H|\Psi|^2dz\equiv\alpha>0. \tag{9}$$

Further taken module of two sides of Formula (9) and applied with relative equations, Formula (9) can be transformed as

$$\int_0^H\left[\left|\frac{2i\hat{f}\bar{v}_z}{\lambda^2-\hat{f}^2}\right|+\left|\frac{2\hat{f}^2\bar{u}_z}{\lambda(\lambda^2-\hat{f}^2)}\right|\right]\cdot\left|\Psi^*\frac{d\Psi}{dz}\right|dz$$
$$+\int_0^H\left[\left|\frac{N^2-k^2\hat{f}^2}{\lambda^2-\hat{f}^2}\right|+\left|\frac{2\hat{f}i\bar{u}_z\bar{v}_z}{\lambda(\lambda^2-\hat{f}^2)}\right|\right]\cdot|\Psi|^2dz\geqslant\alpha. \tag{10}$$

Noticing that the values in the two brackets of Formula (10) are all greater than or equal to zero, and $\left|\Psi^*\frac{d\Psi}{dz}\right|>0$, $|\Psi|^2>0$ applying integration medium theorem, we can get

$$\left(\frac{2\hat{f}\bar{v}_z}{\left|\lambda_c^2-\hat{f}^2\right|}+\frac{2\hat{f}^2\bar{u}_z}{\left|\lambda_c\right|\left|\lambda_c^2-\hat{f}^2\right|}\right)\int_0^H|\Psi^*|\left|\frac{d\Psi}{dz}\right|dz$$
$$+\left(\frac{\left|N^2-k^2\hat{f}^2\right|}{\left|\lambda_d^2-\hat{f}^2\right|}+\frac{2\hat{f}\bar{u}_z\bar{v}_z}{\left|\lambda_d\right|\left|\lambda_d^2-\hat{f}^2\right|}\right)\int_0^H|\Psi|^2dz\geqslant\alpha. \tag{11}$$

Here

$$\begin{cases} \lambda_c = \bar{u}(z_c) - c = \bar{u}_c - c, & z_c \in [0, H], \\ \lambda_d = \bar{u}(z_d) - c = \bar{u}_d - c, & z_d \in [0, H], \end{cases} \tag{12}$$

and $\bar{u}_c = \bar{u}(z_c)$, $\bar{u}_d = \bar{u}(z_d)$, and take $\bar{u}_H = \bar{u}(H)$. Then let

$$\begin{aligned} \tau &= \min(|\lambda_c|, |\lambda_d|, |\lambda_c \pm \hat{f}|, |\lambda_d \pm \hat{f}|) \\ &= \min(|\bar{u}_c - c|, |\bar{u}_d - c|, |\bar{u}_c - c \pm \hat{f}|, |\bar{u}_d - c \pm \hat{f}|). \end{aligned} \tag{13}$$

Here $\tau = |c + \Delta|$, Δ is a real number, it is one of u_c, u_d, $\bar{u}_c \pm \hat{f}$, $\bar{u}_d \pm \hat{f}$. Replacing $|\lambda_c|$, λ_d, and $|\hat{f}^2 - \lambda_c^2|$, $|\hat{f}^2 - \lambda_d^2|$ in the denominator of Formula (11) with τ and τ^2 respectively and considering with Formula (13), it is obvious that denominator will be decreased and the following equation is still tenable

$$\left(\frac{2\hat{f}\bar{v}_z}{\tau^2} + \frac{2\hat{f}\bar{u}_z}{\tau^3}\right)\int_0^H |\Psi^*|\left|\frac{d\Psi}{dz}\right|dz + \left(\frac{|N^2 - k^2\hat{f}^2|}{\tau^2} + \frac{2\hat{f}\bar{u}_z\bar{v}_z}{\tau^3}\right)\int_0^H |\Psi^2|dz \geqslant \alpha. \tag{14}$$

Taking account of $\tau = |c + \Delta|$ and letting $s = k\tau$, then we have $s = k|c + \Delta| = |\sigma + k\Delta|$. Synchronously, substitute $\hat{f}$ with f/k and let $\beta = \int_0^H |\Psi|^2 dz > 0$, $\gamma = \int_0^H |\Psi^*|\left|\frac{d\Psi}{dz}\right|dz > 0$, and multiply Formula (14) with τ^3 and divide it by α then, we obtain that

$$F(s) \equiv s^3 + ps + q \leqslant 0 \tag{15}$$

Here,

$$\begin{cases} p = -(2fk\bar{v}_z\gamma + k^2|N^2 - f^2|\beta)/\alpha = -(2f\overline{U}_z \sin\delta \cdot k\gamma/\alpha + |N^2 - f^2| \cdot k^2\beta/\alpha), \\ q = -(2f^2k\bar{u}_z\gamma + 2k^2f\bar{u}_z\bar{v}_z\beta)/\alpha = -(2f^2\overline{U}_z\cos\delta \cdot k\gamma/\alpha + f\overline{U}_z^2 \sin 2\delta \cdot k^2\beta/\alpha). \end{cases} \tag{16}$$

There exists $p \leqslant 0$, $q \leqslant 0$ while $0^\circ \leqslant \delta \leqslant 90^\circ$, which is the merely case taking account of the following passages and also takes place in real atmosphere frequently.

Now, we will focus on the figure and properties of $F(s)$ under such circumstance. It is obvious that the intercept of $F(s)$ in ordinate direction is equal to $|q|$. Solving the equation $dF(s)/ds = 3s^2 + p = 0$, there will be $s_{1,2} = \pm\sqrt{-p/3}$. For $p \leqslant 0$, s_1 and s_2 are all real numbers. While solving equation $d^2F(s)/ds^2 = 6s = 0$, there will be $s_0 = 0$. Moreover, there is $F(s) \to \infty$, when $s \to \infty$, and while $s \to -\infty$, there is $F(s) \to -\infty$. Thus we can get the figure of $F(s)$ shown in Fig. 1 and know that the cubic equation $F(s) = 0$ has surely exclusive one non-negative real root s_+ which is determined by the coefficients p and q in equation (15). Apparently, the greater the values of $|p|$ and $|q|$ are, the greater s_+ is (Fig. 1). The s which satisfied Formula (15) must also satisfy the following relation without fall

$$s = |\sigma + k\Delta| \leqslant s_+. \tag{17}$$

Thus

$$|\sigma| - |k\Delta| \leqslant |\sigma + k\Delta| \leqslant s_+, \tag{18}$$

and it can be obtained that

$$|\sigma| \leqslant s_+ + |k\Delta|. \tag{19}$$

For Δ is one of u_c, u_d, $\bar{u}_c + \hat{f}$, $\bar{u}_c - \hat{f}$, $\bar{u}_d + \hat{f}$, $\bar{u}_d - \hat{f}$ and here $\hat{f} = f/k$, thus there is

$$ku_c \leqslant k\bar{u}_H + f,\ |ku_d| \leqslant k\bar{u}_H + f,\ |ku_c + f| \leqslant k\bar{u}_H + f,$$
$$ku_c - f| \leqslant k\bar{u}_H + f,\ |ku_d + f| \leqslant k\bar{u}_H + f,\ |ku_d - f \leqslant k\bar{u}_H + f. \tag{20}$$

Here we know

$$|k\Delta| \leqslant ku_H + f. \tag{21}$$

Consider Formula (21), from (19), it can be achieved

$$|\sigma| \leqslant s_+ + |k\Delta| \leqslant s_+ + ku_H + f \equiv R_0, \tag{22}$$
$$\sigma_r^2 + \sigma_i^2 \leqslant R_0^2. \tag{23}$$

From the Formula above, we can see, equation (6) together with boundary condition (5) constitute an eigenvalue problem of ordinary differential equation sets with complex varying coefficients, and its spectrum distributed in a circle in complex plane with radius R_0 and center at O (Fig.2).

When heterotropic instability takes place, Formula (3) implies that σ_i, thus all the unstable spectrum should distribute within an upper semi-circle in complex plane described above which is shown as the shadow part in Fig.2. Therefore, we can obtain the semi-circle theorem of heterotropic unstable spectrum distribution — the unstable spectrum distribute within a semi-circle with center O (origin) and radius R_0 in complex plane. The Formulae (15), (16), and (22) imply that environmental factors such as $\bar{U}_z$, δ, k, N^2, f and H etc. affect the value of R_0.

The semi-circle theorem implies that, when R_0 is fixed, the maximum of $|\sigma_i|$ is R_0 and $\sigma_r = 0$ then. While the maximal propagating speed of perturbation is $R_0 / k = C_{\max}$, that is

$$C_{\max} = R_0 / k = \bar{u}_H + \frac{f}{k} + \frac{\tau_+}{k}. \tag{24}$$

Temporarily, $\sigma_i = 0$ implies a stable perturbation and other phase speed of unstable perturbation is less than such value (Fig.2).

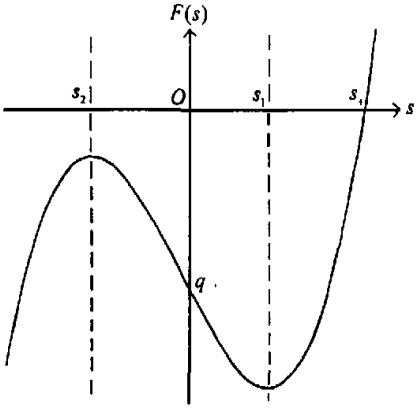

Fig. 1. The picture of function $F(s)$ problem.

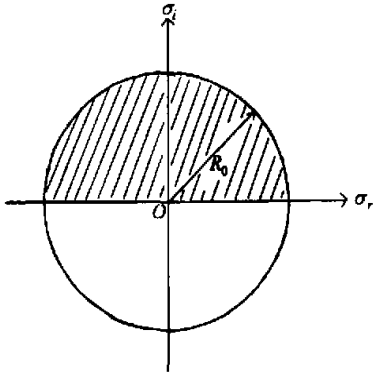

Fig. 2. Spectrum distribution of such eigenvalue problem

Noticing Formula (17) and the real Δ, we can find

$$|\sigma_i| = \sqrt{\sigma_i^2} \leqslant \sqrt{(\sigma_i + k\Delta)^2 + \sigma_i^2} = |\sigma + k\Delta| \leqslant s_+ . \tag{25}$$

Under the circumstances of instability taking place, Formula (3) implies $\sigma_i > 0$. Thus from Formula (25), it can be deduced that

$$\sigma_i \leqslant s_+ , \tag{26}$$

and so, s_+ is the upper bound of growth rate of such heterotropic instability.

4. Estimation of radius of semi-circle and the upper bound of growth rate

Determination of such semi-circle radius and upper bound of growth rate demands the estimated values of p and q, and thus requires the approximation of some non-dimensional quantities such as $k^2\beta/\alpha$ and $k\gamma/\alpha$ above all. Let's consider

$$\begin{cases} \dfrac{k^2\beta}{\alpha} = \dfrac{k^2\int_0^H |\Psi|^2 dz}{\int_0^H \left|\dfrac{d\Psi}{dz}\right|^2 dz + k^2\int_0^H |\Psi|^2 dz} \sim \dfrac{k^2\tilde{\Psi}^2 H}{\dfrac{\tilde{\Psi}^2}{H^2}H + k^2\tilde{\Psi}^2 H} = \dfrac{kH}{kH + \dfrac{1}{kH}}, \\ \dfrac{k\gamma}{\alpha} = \dfrac{k\int_0^H |\Psi^*|\left|\dfrac{d\Psi}{dz}\right| dz}{\int_0^H \left|\dfrac{d\Psi}{dz}\right|^2 dz + k^2\int_0^H |\Psi|^2 dz} \sim \dfrac{k\tilde{\Psi}\dfrac{\tilde{\Psi}}{H}H}{\dfrac{\tilde{\Psi}^2}{H^2}H + k^2\tilde{\Psi}^2 H} = \dfrac{1}{kH + \dfrac{1}{kH}}. \end{cases} \tag{27}$$

Here $\tilde{\Psi}$ is the estimated value of stream function Ψ. Thus, there exists

$$\begin{cases} p = -\left(\dfrac{2k\gamma f\overline{U}_z \sin\delta}{\alpha} + \dfrac{k^2\beta|N^2 - f^2|}{\alpha}\right) \sim -\dfrac{2f\overline{U}_z \sin\delta + kH|N^2 - f^2|}{kH + \dfrac{1}{kH}} \equiv \tilde{p}, \\ q = -\left(\dfrac{2k\gamma f^2\overline{U}_z \cos\delta}{\alpha} + \dfrac{k^2\beta f\overline{U}_z \sin 2\delta}{\alpha}\right) \sim -\dfrac{2f^2\overline{U}_z \cos\delta + kHf\overline{U}_z \sin 2\delta}{kH + \dfrac{1}{kH}} \equiv \tilde{q}. \end{cases} \tag{28}$$

Here $\tilde{p}$ and $\tilde{q}$ are estimated values of p, q, and $\tilde{p} \leqslant 0$, $\tilde{q} \leqslant 0$, within the region ($0^\circ \leqslant \delta \leqslant 90^\circ$).

Noticing the expression of $\tilde{p}$ and $\tilde{q}$ which are merely constituted by circumstance parameter and has no relation with $\tilde{\Psi}$, thus $\tilde{s}_+$ — the estimated value of growth rate upper bound s_+ — is the exclusive non-negative root of cubic equation

$$\tilde{F}(\tilde{s}) = \tilde{s}^3 + \tilde{p}\tilde{s} + \tilde{q} = 0. \tag{29}$$

Formula (29) can also be rewritten on the non-dimensional pattern, thus divides it with N^3 and takes s/N as relative growth rate $\hat{s}$, the ratio of unstable growth rate and $|N|$. It is understood that convective instability will take place if $N^2 < 0$ (that is also called geopotential instability while substituting N with N_w), and the growth rate of such instability is $|N|$. So, the relative growth rate is exactly the one compared to convective (geopotential) instability and the greater its value is, the easier the heterotropic instability will take place. Now, there is

$$\hat{F}(\hat{s}) = \hat{s}^3 + \hat{p}\hat{s} + \hat{q} = 0. \tag{30}$$

Here

$$\hat{p} = -\frac{2 \cdot \frac{f}{\overline{U}_z} \cdot \frac{1}{Ri}}{\cdot \sin\delta + kH \cdot \left|1 - (\frac{f}{N})^2\right|} kH + \frac{1}{kH}$$

$$= -\frac{2 \cdot R_f \cdot \sin\delta + kH \cdot \left|1 - (\frac{f}{N})^2\right|}{kH + \frac{1}{kH}} \tag{31}$$

$$\hat{q} = -\frac{2 \cdot \frac{f}{\overline{U}_z} \cdot \frac{f}{N} \cdot \frac{1}{Ri}}{\cos\delta + kH \cdot \frac{f}{N} \cdot \frac{1}{Ri}} \cdot \sin 2\delta / kH + \frac{1}{kH}$$

$$= -R_f \cdot \frac{2 \cdot \frac{f}{N} \cdot \cos\delta + kH \cdot \frac{\overline{U}_z}{N} \cdot \sin 2\delta}{kH + \frac{1}{kH}} \tag{32}$$

$\hat{p}$ and $\hat{q}$ in Formula (30) are determined by non-dimensional parameter $f/N, \overline{U}_z/N, kH$ R_f and δ, and here $R_f = \frac{f}{\overline{U}_z Ri} = \frac{f\overline{U}_z}{N^2}$, $Ri = N^2/\overline{U}_z$. The discussion of the properties of $\tilde{F}(\tilde{s})$ and $\hat{F}(\hat{s})$ are similar to that of $F(s)$ and is omitted here. $\tilde{p}, \tilde{q}$ or $\hat{p}, \hat{q}$, can be determined after the parameter $N^2, f, \overline{U}_z, \delta, k, H$ or $f/N, \overline{U}_z/N, kH, R_f, \delta$, are determined and equation (29) or (30) can be solved consequently. Thus the estimation of upper bound of growth rate $\tilde{s}_+$ or relative growth $\hat{s}_+$ can be obtained.

Extending the above discussion as for the non-dimensional case, the greater $|\hat{p}|$ and $|\hat{q}|$ is, the greater the upper bound relative growth rate $\hat{s}_+$ will be (Fig 1). The second absolute term in Formula (31) can be omitted $(f/N)^2 \ll 1$ generally. The expression of $\hat{p}, \hat{q}$ implies that the greater $\overline{U}_z$ and f are and the less N^2 is, then the greater $f/N, \overline{U}_z/N$, and R_f will be, and so does $|\hat{p}|$ $|\hat{q}|$, and $\hat{s}_+$. Therefore, the reinforcing vertical shear of wind, the decreasing of stratified stability and the increasing of latitude have positive contribution to increasing the upper bound of growth rate of relative instability.

Formulae (31) and (32) imply that both $|\hat{p}|$ and $|\hat{q}|$ have the expression of $(a + bx)/(x + 1/x) = \xi(x)$, and here x stands for $kH, a > 0, b > 0$. The derivative of ξ to x can be written as

$$\frac{d\xi(x)}{dx} = \frac{a(1 - x^2) + 2bx}{(1 + x^2)^2} \tag{33}$$

and $d\xi(x)/dx > 0$ within the region $0 < x < 1$. Formula (33) shows that $\xi(x)$ decreases with the decreasing x within such region. It can be deduced that $|\hat{p}|$ and $|\hat{q}|$ decrease with the increasing perturbation wavelength L when $kH < 1$ which indicates $L > 2\pi H$, and so does $\hat{s}_+$. Here into H is about 10 km and so $2\pi H$ is about 63 km. Furthermore $\hat{p} \to 0$ and $\hat{q} \to 0$ while $L \to \infty$, and from this, we can get $\hat{s}_+ \to 0$. On the other hand, the higher the model top is, the greater $\hat{s}_+$ will be if L is fixed. But until now the effect of δ to $|\hat{p}|$ and $|\hat{q}|$ is under discussion for its illegibility.

Dimensional case will be discussed similarly. The increase in vertical shear of wind and

latitude has the positive effect on the increasing of upper bound of unstable growth rate, as to the perturbation with wave length greater than $2\pi H$, the variation trend of its upper bound $\tilde{s}_+$ is similar to the case above. But it is different to non-dimensional one as the greater N^2 is, the greater $|\tilde{p}|$ is and so does $\tilde{s}_+$, thus perform the positive contribution to the growing of upper bound of instability growth rate, which results from the fact that greater value of N^2 benefits the accumulation of unstable energy. In general, greater value of N^2 is not benefitial to instability, but plenty of energy accumulated will be released and the disturbance will develop up quickly once the instability takes place.

$\tilde{R}_0$ the estimated value of radius R_0 of semi-circle in which spectrum distribution — can be calculated as

$$\tilde{R}_0 = \tilde{s}_+ + ku_H + f. \tag{34}$$

Consider parameter N^2, f, $\bar{U}_z$, and H as $0.8\times 10^{-5}\,s^{-2}$, $0.9\times 10^{-4}\,s^{-1}$, $4\times 10^{-3}\,s^{-1}$, and 10 km (the values taken from reference Zhang and Zhang (1992) and Zhang (1988a, b), ideographic computation is performed. Table 1 shows $\max \tilde{s}_+$ — the maximum of estimated value of upper bound of growth rate in different angles correspond to horizontal wave length L (unit: km) and $\max \tilde{R}_0$ (unit: $10^{-4}\ s^{-1}$), the maximum estimate value of semi-circle radius and the angle δ (unit: degree).

Table. 1. $\max\tilde{s}_+$, $\max\tilde{R}_0$ and δ corresponding to different perturbation wavelength L

L	20	50	100	200	300	500	800	1000	2000
$\max\tilde{s}_+$	28.070	23.540	16.637	10.088	7.360	4.987	3.557	3.056	1.976
$\max\tilde{R}_0$	154.63	74.706	42.670	23.555	16.638	10.934	7.599	6.469	4.133
δ	53	53	55	56	57	57	56	56	55

Table 1 shows that the greater L is, the less the $\max \tilde{s}_+$ will be, which is consistent with the case above. Furthermore, $\max \tilde{s}_+$ of perturbation with $L=20$ km is 14.2 times more than that of perturbation with $L=2000$ km. So, the upper bound of growth rate in meso-β scale is great enough to catch people's attention. Further calculation also shows that the maximum value of $\max \tilde{s}_+$ is $29.145\times 10^{-4}\ s^{-1}$ and $\delta=45^\circ$ while $L=2$ km which tally with the cumulus scale. While $L\to 0$, there is $\max \tilde{s}_+ \to 29.131\times 10^{-4}\ s^{-1}$ and then $\alpha=45^\circ$. Furthermore, $\tilde{R}_0$ and $\tilde{s}_+$ in Table 1 has the same tendency except for their values that result from the effects of $ku_H + f$, which is also the effect of advection and geostrophic parameter. But with the variation of wavelength L, angle δ has a process of increasing first and decreasing then and obtains its maximum at 300 km.

5. Conclusions

Spectrum distribution of heterotropic perturbation and upper bound of growth rate of its instability are discussed in the paper and the following main conclusions are made.

(1) Unstable spectrum of heterotropic perturbation distributed in an upper semi-circle with radius R_0 and regarding origin as center of the circle in complex plane, which is also the exact semi-circle theorem of perturbation spectrum distribution.

(2) The less the horizontal scale of disturbance is, the higher the model top located, the greater the estimated value of upper bound of growth rate of such instability will be.

(3) The reinforcment of vertical wind shear and the increase of latitude have positive effect on the enhancement of upper bound of growth rate.

(4) The decrease of stratified stability will cause the increase of upper bound of relative

growth rate of instability, and the decreasing of upper bound of growth rate for going against the energy accumulation.

There is merely estimation of upper bound of unstable growth rate of heterotropic perturbation, but there is no indication that instability will take place consequently and the real growth rate can reach such a great value. Furthermore, it is difficult to obtain the analytical growth rate and the effect of environment on it, which is also an important aspect to be investigated in the future. The last one, effect of β should be considered as to the perturbation with scale greater than 1000 km, which is omitted like Eady (1949) for the convenience of theoretical study, and the case of considering β effect will be discussed later.

REFERENCES

Charney, J. G., 1947: The dynamics of long waves in a baroclinic westerly current. *J. Meteor.*, **4**, 135–162.

Eady, E. T., 1949: Long waves and cyclone waves. *Tellus*, **1**, 33–52.

Wang Liqiong, 2000: The study on meso-instability. The Paper of Master Degree of Science and Engineering University of P.L.A., Nanjing, China (in Chinese).

Xu Zixiu, and Wang Pengyun, 1989: The character and mechanism analysis of mesoscale rain belt in front of cold front. *Acta Meteorologica Sinica*,**47**, 199–206 (in Chinese).

Zhang Kesu, 1988a: Mesoscale instability of baroclinic stream I: Symmetry instability. *Acta Meteorologica Sinica*,**46**(4), 258–268 (in Chinese).

Zhang Kesu, 1988b: Mesoscale instability of baroclinic stream II: Transversal instability. *Acta Meteorologica Sinica*,**46**(4), 385–391 (in Chinese).

Zhang Lifeng, and Zhang Ming, 1991: WAVE-CISK and non-geostrophic instability propagating along the shear stream. *Journal of Air Force Institute of Meteorology*, **12**(2), 56–63 (in Chinese).

Zhang Lifeng, and Zhang Ming, 1992: WAVE-CISK and symmetry instability. *Chinese Journal of Atmospheric Science*, **16**, 669–676 (in Chinese).

Zhang Lifeng, Wang Liqiong, and Zhang Ming: Instability of non-geostrophic eddy wave in vertical shear stream. *Chinese Journal of Atmospheric Sciences*, to be published (in Chinese).

Zhang Ming, and Zhang Lifeng, 2000: The study on the instability of -mesoscale eddy wave. Review of atmospheric sciences and look into its future at the beginning of 21st century. *Proceedings Third Conference on Leading Course of Atmospheric Sciences*, China Meteorological Press, 149–152 (in Chinese).

Zhang Ying, and Zhang Ming, 1995: Numerical experiment of linear and non-linear symmetry instability. *Acta Meteorologica Sinica*,**53**, 225–231 (in Chinese).

Zhang Ying, and Zhang Ming, 1998: Numerical study on linear and non-linear transversal instability. *Acta Meteorologica Sinica*,**56**(4), 447–457 (in Chinese).

斜交型不稳定谱点分布侧半圆定理及其增长率上界的估计

张 铭 张立凤

摘 要

本文对斜交型扰动不稳定谱点的分布做了理论分析，得到了该谱点分布的半圆定理—该谱点分布在复平面上以原点为圆心以 R_0 为半径的上半平面上，同时还对该不稳定增长率的上界作了估计。发现水平尺度越小，模式顶越高则该估计值越大；垂直风切变的增大和纬度的增高对该增长率的增大有正贡献；当层结稳定度减小时，最大增长率随相对最大增长率得增大而减小。

关键词： 斜交型扰动，半圆定理，增长率